13th Australasian Fluid Mechanics Conference
Monash University, Melbourne, Australia
13-18 December 1998

LARGE SCALE FLAPPING OF SEPARATED FLOW

Andreas FOURAS and Julio SORIA

Department of Mechanical Engineering
Monash University, Clayton, Victoria, AUSTRALIA

ABSTRACT

A novel image recording technique coupled with adaptive cross-correlation digital PIV analysis has been applied to the measurement of unsteady separated flow over a blunt flat plate at a Reynolds number of 1000. A bubble fraction function derived from the spatial velocity field is defined and used to measure the unsteady separated bubble size. The results presented in this paper include spectra of the vorticity and of this newly defined bubble fraction function.

INTRODUCTION

Recent technological advances in optical and computer hardware allow the acquisition of a sufficient number of digital images at a rate that allows spectral analysis of the resultant PIV data. Although PIV might never fill the role played by single point measuring techniques such as hot-wire anemometry, this is an important development in experimental fluid mechanics. Spectra of vorticity and other spatially derived quantities can only be determined using spatial velocity field measurement methods such as PIV.

EXPERIMENTAL APPARATUS

The experiments for this investigation were conducted in a vertical closed circuit water tunnel. The results presented in this paper pertain to the separated and reattaching flow over a blunt leading edge flat plate. The model used in this investigation is a $23.2mm$ thick (H) machined and polished acrylic test plate with equal length to height and aspect ratios of 10.7. The free stream velocity was $30.7mm.s^{-1}$ corresponding to a Reynolds number (Re_H) of 1000. The free stream turbulence intensity at this velocity was less than 0.1%.

The flow was seeded with Potters Industries $16\mu m$ diameter silver coated hollow glass spheres with a nominal specific gravity of 1.1. These particles were illuminated by pulsed laser sheets. The pulsed light sheets were generated by two independent Spectra Physics Quanta Ray GCR170 Nd:YAG lasers producing $6ns$ pulses, each with a maximum energy output of $400mJ$ at $532nm$. The pulsing rate of the laser is computer controlled with a maximum repetition rate of $12Hz$. The lasers were operated at orthogonal states of polarisation which allowed, the beam paths to be combined using a polarising beam splitter plate operated at Brewster's angle.

The digital image acquisition was performed using a Kodak MegaPlus XHF digital camera with a $1018pixel \times 1008pixel$ (px) CCD array capable of a maximum acquisition rate of 30 frames per second. This camera is coupled to an IC-PCI digital frame grabber board with $2MB$ of on-board RAM allowing direct acquistion of up to two images at $30Hz$. For longer acquisition sequences images are transferred to PC-RAM or hard disk. Timing and control of the lasers and the digital camera was performed using a Pentium based PC. To enable longer series of digital images to be acquired, the PC was equipped with a dedicated $2GB$ hard drive enabling acquisition of up to 2000 full frames at a maximum acquisition rate of $1.98Hz$.

A NEW METHOD FOR RECORDING TWO NON-OVERLAPPING IMAGES

A new image recording technique which permits the recording of two non-overlapping, single-exposed images onto the same frame has been developed. This is achieved by masking half of the exposable image plane, such that it is imaged onto only half of the recording medium. The second exposure of the same object region is then imaged onto the masked half of the recording medium using an optical image shifting technique. This new recording method results in two non-overlapping, single-exposed images of the same physical region in the flow, which are subsequently amenable to cross-correlation digital PIV (CCDPIV) analysis.

A purely optical means is used in this study to achieve the image shifting, by utilising the polarisation state of laser light Kostas *et al.* (1996). The necessary components for implementation of this image shifting technique are depicted in Fig. 1.

The primary component in this system is a polarising beam splitter cube. This cube splits the beam path according to the polarisation state of the light scattered by the seeding particles in the flow. Ver-

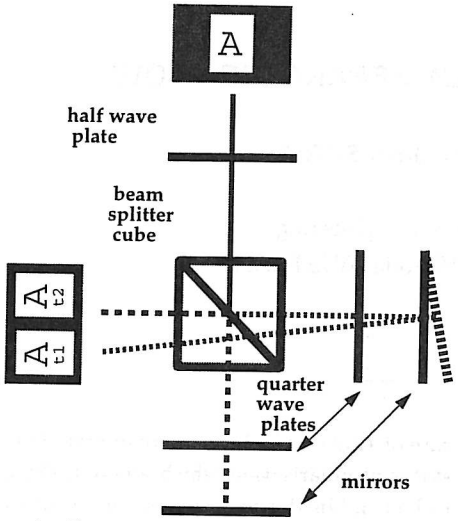

Figure 1: Image shifting and image acquisition components

tically polarised light is permitted to pass directly through the cube. It then passes through a quarter wave plate, is reflected by a mirror and passes back through the quarter wave plate. Two traverses through a quarter wave plate rotate the polarization state by 90^o. This light now being of horizontal polarisation is transmitted through the cube directly into the camera.

Initially horizontally polarised light is first transmitted through the cube and then deflected by it, before reaching the camera. Micrometer adjustment of the alignment of either of the mirrors behind the quarter wave plates can independently shift the image. For this optical image shifting technique to work, it is essential that the scattered light from the particles retains the incident laser polarisation state. The seeding particles used in this investigation had this charateristic.

This image acquisition technique has been termed *Half Frame Optical Image Shifting* (HFOIS). The primary disadvantage of HFOIS is that each images is only half the potential size in one of the dimensions. However, this is heavily outweighed by the fact that two single-exposed, non-overlapping images can now be recorded onto the same medium (*e.g.* high resolution film or a CCD array) with an arbitrary time delay between their recording.

The potential ability to perform CCDPIV analysis of non-overlapping, single-exposed images recorded on high spatial resolution film or digital CCD with an arbitrary time delay between exposures is a direct result of the nature of the novel image recording method with optical image shifting. The absence of any moving parts in the image shifting permits the measurement of high speed flows and event triggered image recording onto high spatial resolution media without *a priori* assumptions of the flow.

PIV ANALYSIS

Standard CCDPIV Analysis (Adrian(1986)) is limited in its measurement capabilities by a combination of two factors. The first results from the fact that the largest reliable measurement that can be made using CCDPIV is approximately equal to one quarter of the size of the interrogation window. The second contributing factor arises when larger interrogation windows need to be used to measure large displacements, in this case the larger the interrogation windows result in a larger sampling distance between the independent velocity measurements.

A novel CCDPIV analysis method that allows for a greatly increased spatial resolution and larger dyanmic velocity range was proposed by Soria(1996). The main idea of this technique is that a large interrogation window is used to estimate the local displacement. Then in a iterative process successively smaller windows are used but with the interrogation window in the second exposed image offset by a displacement equal to the estimated displacement determined from the previous larger window.

The only limitation to the spacing of independent measurements is the size of the smallest window (SWS_{min}) that will result in accurate results. This minimum window size is determined by the necessity to contain at least 5 particle images Soria(1996) within it. In the present investigation the use of this adaptive CCDPIV analysis technique results in an increase of the spatial resolution by a factor of 4.0.

RESULTS AND DISCUSSION

The data presented in this paper is extracted from a single time series of images that was acquired by capturing to the hard disk of the acquisition computer at a rate of $1.98Hz$. This corresponds to a ΔT between pairs of images of $505ms$ or a non-dimensionalised time of $\Delta T' = \Delta T U_\infty$ / H = 0.668. All other quantities are either non-dimensionalised by U_∞, H or an appropriate combination of U_∞ and H .

This acquired PIV time series contains 1049 vector fields. Using the adaptive CCDPIV analysis technique with a sampling window size of $32px$ and a velocity sampling spacing of $16px$, 61 $\times$ 25 vectors were measured in each velocity field. The vorticity was calculated using 13 velocity data points in the χ^2 technique described in detailed in Fouras & Soria(1998).

The instantaneous velocity and vorticity fields provide the spatial structure of the flow while the time series of these fields allows the temporal evolution of the spatial structure to be invetigated. The vorticity data is the focus of this study as it is Gallilean invariant quantity, and hence any conclusions derived from it are indpendent of an interial observer.

A number of complex aspects of this highly un-

steady separated flow are depicted in Fig. 2. In this figure the leading edge of the plate is at the origin with the free stream flow in the direction of increasing x. The data in Fig. 2 is a realisation of a full cycle of the rolling up of the shear layer. Its weakening in intensity with growth is observed in during its temporal evolution. In the fourth frame the rolled up sheet is seen to contact the wall. Also of interest is the development of the wavy instability of the shear layer that can be seen in the last two frames.

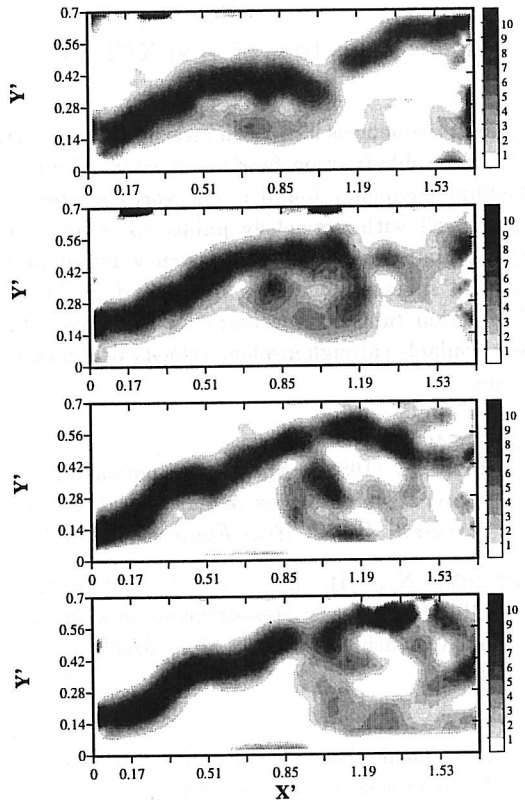

Figure 2: The evolution of the normalised spanwise vorticity ($\omega_z' = \omega_z H/U_\infty$) showing one complete shedding cycle.

The large scale flapping motion observed in previous investigations of this flow geometry has been captured with approximately 50 velocity fields per cycle. Fig. 3 shows the instantaneous in-plane velocity field at two extremes of the flapping cycle. In the first frame the bubble covers approximately 86.0% of the flow region region shown while in the the second frame the area covered by the sepration bubble only covers approximately 25.9% of the this region.

In order to quantify the bubble position and its size, two definitions of bubble position were investigated. In one method the bubble was defined in a similar way to a boundary layer. The bubble was defined to be the region between the plate and the wall-normal distance were the velocity first reached $0.99U_\infty$. In the other method the bubble was de-

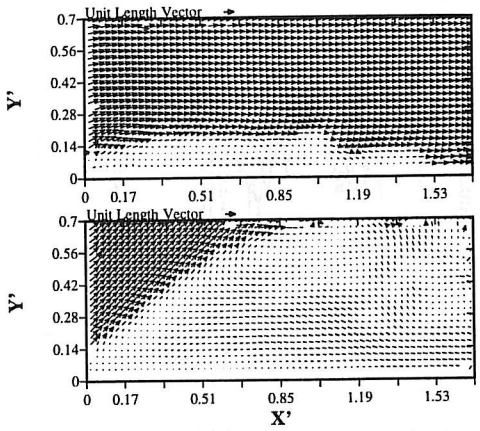

Figure 3: Normalised velocity vector field at two extremes of the flapping cycle.

fined to be the region between the plate and the wall-normal distance to the point of maximum spanwise vorticity magnitude. In the majority of cases both definitions gave exactly the same result. However, in a small number of cases where small strong concentrated spanwise vorticity was observed inside the bubble the second method resulted in a bubble boundary definition which resided inside these strong vorticity structures, and thus excluding large regions of the recirculating flow of the bubble. For this reason the velocity based criterium was preferred to quantify the bubble domain.

The ability to quantify the flapping of the bubble is one of the distinct advantages of using PIV over pointwise measurement techniques. This measurement requires instantaneous velocity vector field measurements. A bubble function which is a binary number used to define whether a measurement station was inside or outside of the separation bubble at an instant. A value of 0 is used to represent being inside of the bubble and a value of 1 is used to represent being outside of the bubble.

A bubble fraction function, defined as the spatial average value of the bubble function over the entire analysis region, is used to follow the large scale motion or flapping of the flow. A typical time series of this function is shown in Fig. 4.

Fig. 5 shows the corresponding spectrum of the time series shown in Fig. 4. A clear broad spectral peak is observed at 0.035. The frequency of the broad spectral peak is a considerably lower than the broad spectral peak found by Eaton & Johnston(1982), Kiya & Sasaki(1983) and Cherry *et al.* (1984) at approximately 0.6 (universally found to be the shedding frequency) and frequencies of about one third to one fifth of this. It is suspected that the quoted frequency in those studies is the second harmonic of the flapping frequency. This is somewhat substantiated by the admission in Cherry *et al.* (1984) that there is

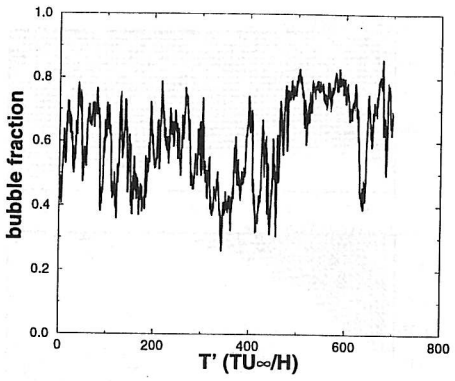

Figure 4: Time trace of bubble fraction function.

a unsteadiness in the flow with a period of order of or greater than the entire time records. However, in Cherry *et al.* (1984) a spectral peak at 0.035 is found in the measurements for x/H = 0.15 and this spectral peak is associated with the flapping of the shear layer.

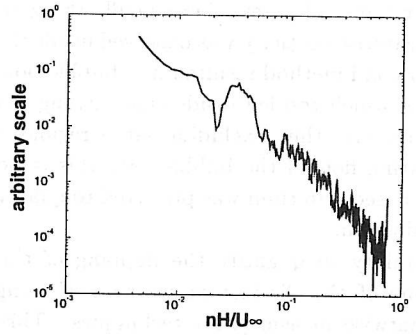

Figure 5: Spectrum of bubble fraction function

Fig. 6 shows the average of all vorticity spectra calculated at X/H = 0.13. Marked on Fig. 6 are the flapping and shedding frequency peaks. The flapping peak at 0.035 is in excellent agreement with the peak shown in Fig. 5 and the results of Cherry *et al.* (1984). The value of 0.6 for the shedding peak is also in excellent agreement with previously published values in Eaton & Johnston(1982), Kiya & Sasaki(1983) and Cherry *et al.* (1984).

Present in both of these spectra are the strong harmonics of the flapping frequency. It is the second of these that may have been misinterpreted by previous researchers as the flapping frequency.

CONCLUSIONS

The unsteady separated flow over a blunt flat plate at a Reynolds number of 1000 has been measured using the combination of a new image acquisition technique and adaptive cross-correlation PIV analysis.

A bubble fraction function describing separation bubble size from velocity vector field data has been introduced. The vortex shedding and separation bubble

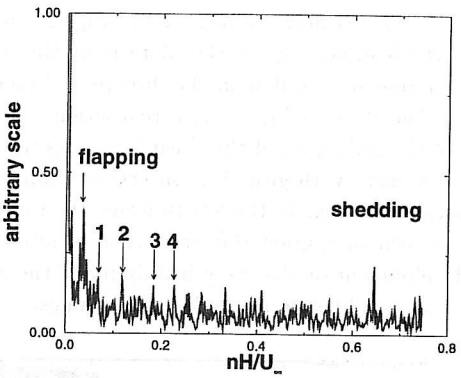

Figure 6: Spectrum of ω_z at X/H = 0.13

flapping frequencies have been measured using vorticity and bubble fraction function spectra. The vortex shedding frequency found in the vorticity spectrum agrees well with previously published results. The separation bubble flapping frequency found in the vorticity spectrum matches that found in the bubble fraction function spectrum. This latter data is only available through in-plane velocity field measurements.

REFERENCES

ADRIAN, R. (1986). Multi-point optical measurements of simultaneous vectors in unsteady flow - A review. *Int. J. Heat Fluid Flow* **7**, 127–145.

CHERRY, N., HILLIER, R., & LATOUR, M. (1984). Unsteady Measurements in a Seperated an Reattaching flow. *J. Fluid Mech.* **144**, 13–46.

EATON, J. & JOHNSTON, J. (1982). Turbulent Shear Flows, chapter 3: Low Frequency Unsteadiness of a Reattatching Shear Layer. *Springer.*

FOURAS, A. & SORIA, J. (1998). Accuracy of out-of-plane vorticity measurements using in-plane velocity vector field data. *Exp. Fluids (accepted for publication).*

KIYA, M. & SASAKI, K. (1983). Structure of a Turbulent Seperation Bubble. *J. Fluid Mech.* **137**, 83–113.

KOSTAS, J. D., FOURAS, A., & SORIA, J. (1996). The Application of Image Shifting to PIV. In *1st Australian Conference on Laser Diagnostics in Fluid Mechanics and Combustion* Sydney Australia.

SORIA, J. (1996). An investigation of the near wake of a circular cylinder using a video-based digital cross-correlation particle image velocimetry technique. *Experimental Thermal and Fluid Science* **12**, 221–233.